Supersolidus Liquid-Phase Sintering of Prealloyed Powders

RANDALL M. GERMAN

A model is derived for the sintering densification of prealloyed particles that form internal liquids when heated over the solidus temperature. The model considers the powder size, composition, and microstructure, as well as the processing conditions of green density, heating rate, maximum temperature, hold time, and atmosphere. Internal liquid forms and spreads to create an interparticle capillary bond that induces densification during sintering. Densification is delayed until the particles achieve a mushy state due to grain boundary wetting by the internal liquid. This loss of rigidity and concomitant densification of the semisolid particles depends on the grain size and liquid quantity. Viscous flow is the assumed densification mechanism, where both viscosity and yield strength vary with the liquid content and particle microstructure. Densification predictions are compared to experimental data, giving agreement with previously reported rapid changes in sintered density over narrow temperature ranges. The model is tested using data from steels and tool steels of varying carbon contents, as well as boron-doped stainless steel, bronze, and two nickel-based alloys.

I. INTRODUCTION

THE formation of a liquid during sintering is a common technique to enhance densification. Typically, liquid-phase sintering begins by mixing two or more small powders of differing compositions.[1] On heating, one powder melts or reacts to form a liquid between the particles that engulfs the more refractory phase. If the particle size is small, then capillary forces from the wetting liquid enhance densification.[2] The process consists of several overlapping steps involving solid-state diffusion, particle rearrangement, solution reprecipitation, and solid skeleton densification. After sintering, the product is a composite of refractory grains interlaced with a solidified liquid. To obtain a significant advantage from the liquid requires a large capillary force from the wetting liquid, which in turn mandates a small initial particle size, often in the range of 1 μm or less.

A variant to traditional liquid-phase sintering is to use alloy powders, which are heated to a temperature between the liquidus and solidus. The liquid forms inside the particles and spreads to the particle contacts, resulting in a capillary force acting on the semisolid particles. This process is termed supersolidus liquid-phase sintering (SLPS).[3] Densification is rapid once sufficient liquid forms to fragment the particles into individual grains. In this case, even large particles exhibit rapid densification. The widespread implementation of powder atomization technologies capable of producing large quantities of alloy powders in the 20- to 250-μm size range provides a new opportunity for SLPS. Normally, these powders are too coarse for use in traditional liquid-phase sintering, but they prove ideal for supersolidus sintering. Additionally, the full density, high alloy, and homogeneous microstructure of the sintered products result in higher mechanical properties as compared to traditional powder metallurgy products.

Densification during SLPS is analogous to viscous flow sintering, because the semisolid particles turn mushy and flow once liquid spreads along the grain boundaries. The viscosity decreases as the liquid volume fraction increases, so more liquid makes for faster sintering, but less dimensional precision. Consequently, temperature (which controls the solid-liquid ratio) is a main determinant of sintered density and dimensional precision. As illustrated by the data in Figure 1, densification depends on attaining a critical temperature.[4] This plots the sintered density of a 30-μm nickel-based alloy powder *vs* sintering temperature for compacts initially 62 pct dense. Densification occurred over a narrow temperature range. Prolonged holds in the presence of the liquid phase result in microstructure coarsening with concomitant property decrements. Further, sintering above the critical temperature leads to formation of excess liquid and compact distortion.

Unfortunately, fundamental understanding of SLPS is sketchy and predictive models lag far behind practice. An improved understanding would assist in developing new alloy powders or sintering cycles better suited to the process. Accordingly, a model is constructed based on earlier calculations and observations.[3–7] This model relies on recent capillary force and viscous flow densification calculations as applied to semisolid structures.[8,9] Viscosity for the semisolid particles is estimated using rheocasting data, with consideration of the liquid-solid ratio, structural connectivity, temperature, and grain size. Finally, comments are offered on the problem of component shape preservation during sintering.

II. ALLOY EFFECTS

Liquid formation on heating an atomized alloy particle involves the reverse of solidification. Liquid nucleates at the sites which solidified last in atomization. Observations on quenched particles show liquid located along grain boundaries, inside grains, and at pendular necks between particles.[10,11] Figure 2 is a micrograph of a partially sintered bronze powder with liquid at these three locations. On initial heating, phase diagrams prove inaccurate as a basis for estimation of the solid-liquid ratio. Particle formation during atomization is far from an equilibrium solidification event; accordingly, liquids might form at

RANDALL M. GERMAN, Brush Chair Professor in Materials, is with the Department of Engineering Science and Mechanics, The Pennsylvania State University, University Park, PA 16802-6809.

Manuscript submitted September 13, 1996.

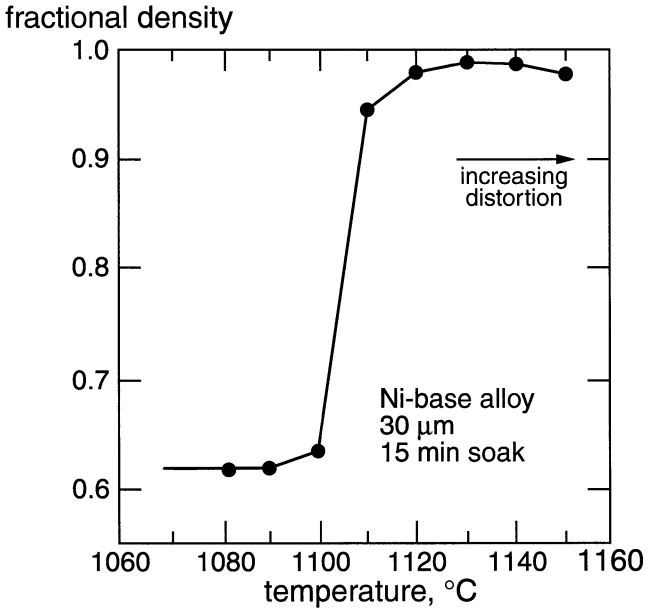

Fig. 1—The sintered fractional density *vs* sintering temperature for a 30-μm Ni-Cr-Co alloy powder processed from a green density of 0.62 using a hold time of 15 min at each temperature. The dramatic change in sintered density over a narrow temperature range is characteristic of liquid-phase sintering with prealloyed powders.

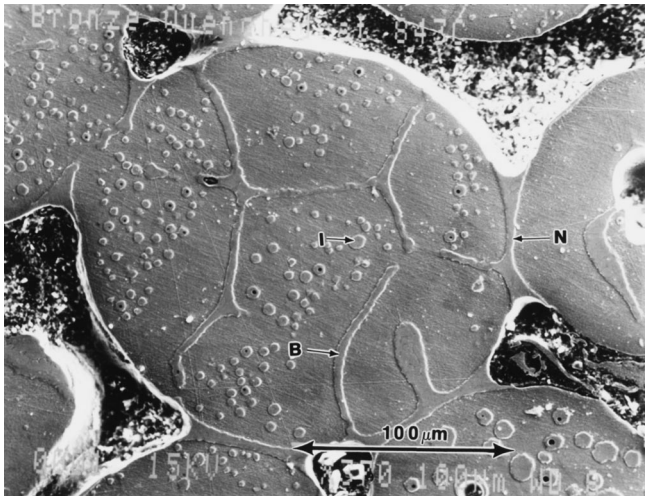

Fig. 2—A quenched microstructure of prealloyed bronze particles undergoing supersolidus liquid-phase sintering. The liquid phase is apparent at three locations—the interparticle necks ''N,'' along the grain boundaries ''B,'' and at sites inside the grains. ''I.''

temperatures 50 °C lower than indicated by the phase diagram. For example, the 132-μm bronze powder (90Cu-10Sn) pictured in Figure 2 exhibited first liquid-phase sintering densification 25 °C below the equilibrium temperature.[12] Once liquid forms, the microstructure converges toward equilibrium and phase diagrams prove useful in estimating the stable solid-liquid ratio and final densification.

Assuming a linear relation between the liquidus and solidus temperatures and composition allows estimation of the solid volume fraction as a function of temperature. The solidus and liquidus temperatures (T_S and T_L) change linearly with alloy composition X_A as follows:

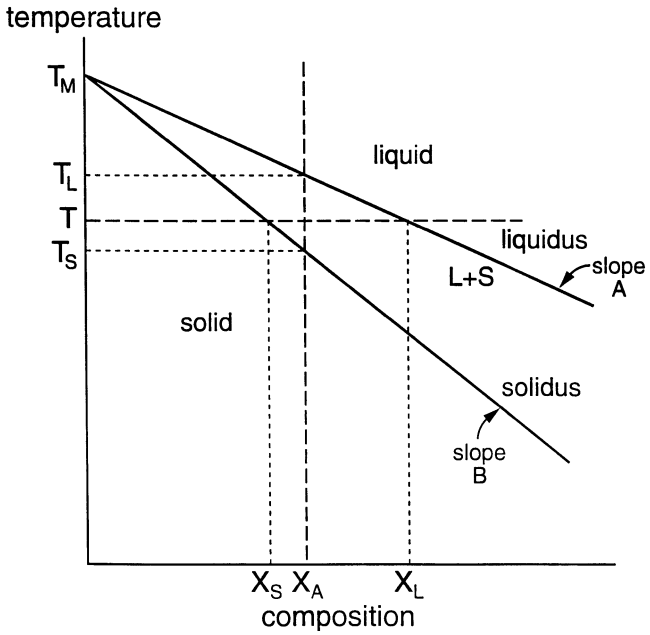

Fig. 3—A schematic phase diagram showing the solidus and liquidus as straight lines, providing a simple means to estimate the effect of temperature on the liquid content and densification for an alloy of composition X_A.

$$T_L = T_M + AX_A \quad [1]$$

$$T_S = T_M + BX_A \quad [2]$$

where T_M is the baseline melting temperature, as sketched in Figure 3; X_A is the alloying content on a weight basis; and A and B are the slopes. Actual alloy melting behavior may be more complicated, but usually is not documented such that we can invoke any more realistic model. With the assumed linear relation, the compositions at the liquidus and solidus lines (X_L and X_S, respectively) for any composition and temperature are given as

$$X_L = \frac{T - T_M}{A} \quad [3]$$

$$X_S = \frac{T - T_M}{B} \quad [4]$$

The tie-line between these two compositions allows calculation of the solid mass fraction M_S for the particle at a given sintering temperature T:

$$M_S = \frac{X_L - X_A}{X_L - X_S} \quad [5]$$

In turn, the volume fraction of solid Φ depends on the solid mass fraction and the densities of the solid ρ_S and liquid ρ_L phases as follows:

$$\Phi = \frac{M_S/\rho_S}{M_S/\rho_S + (1 - M_S)/\rho_L} \quad [6]$$

Thus, for a given alloy composition and sintering temperature, the solid volume fraction inside the alloy particles can be calculated from the liquid and solid densities, if the solidus and liquidus temperature dependencies are known.

The liquid phase has three possible locations during sintering (as evident in the quenched microstructure shown in

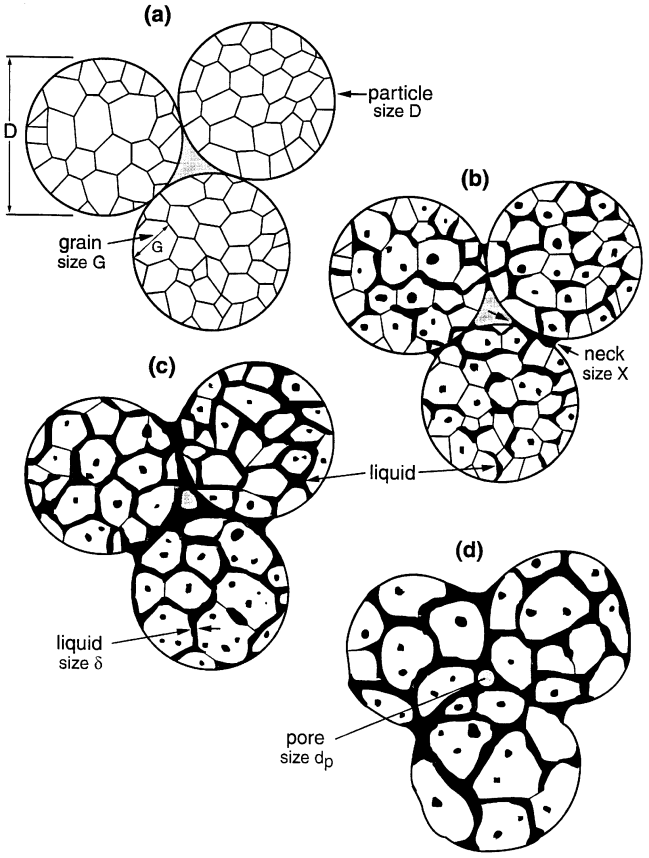

Fig. 4—The conceptual outline of SLPS densification for three particles: (*a*) initial particle packing, (*b*) formation of initial liquid with insufficient wetting of grain boundaries for densification, (*c*) viscous flow densification of semisolid particles, and (*d*) final stage densification with closed, spherical pores.

Figure 2): at the interparticle neck *N*, along grain boundaries inside the particles *B*, and at pockets located inside the grains *I*. The liquid located at the interparticle necks provides the capillary force for densification, while the liquid located on the grain boundaries lubricates grain sliding during densification. From quenched micrographs, it appears the necks form early, but densification is delayed by the particle rigidity. Liquid that forms inside the grains plays no discernible role in densification. If a high fraction of internal liquid forms, then densification is delayed to a higher total liquid content. A widely varying liquid content needed for densification is noted in a prior review.[3] Such variation is probably due to differences in composition and powder fabrication conditions that influence the fraction of liquid forming internal pockets.

III. SINTERING MICROSTRUCTURE

A schematic of the sintering microstructure and its evolution is given in Figure 4. Key features are associated with the particles, grains, necks, grain boundary liquid, and pores. The grain size is G, particle size is D, neck size between particles is X, and width of grain boundary liquid film is δ. As densification progresses, spherical pores form with diameters of size d_p. For this analysis, the film thickness is assumed constant until most of the grain boundaries are wetted. This is in rough agreement with experimental observations, realizing that late in the process, grain growth leads to progressive thickening of the grain boundary films.[7] The particles are assumed to be spheres and the grains are assumed to be polygons. Initial concepts suggested a tetrakaidecahedron grain shape.[5] However, the grain coordination number declines as the relative liquid content increases.[13,14] Based on these earlier calculations, the variation in grain coordination number N_G can be estimated from the solid volume fraction Φ for a zero dihedral angle as

$$\log_{10}(N_G) = 1.15 + 1.25 \log_{10}(\Phi) \qquad [7]$$

The total liquid volume is represented by the sum $V_L = V_B + V_N + V_I$, where V_B, V_N, and V_I designate the liquid volumes (per particle) at the boundary, neck, and grain interior, respectively. The only liquid on the free surface of the particles occurs where the grain boundaries emerge from inside the particles. This assumes grain boundary wetting prevents liquid egression to the surface. With respect to a single spherical particle, the liquid volume fraction tied up in these three forms gives the solid volume fraction as

$$\Phi = 1 - \left(\frac{V_B + V_N + V_I}{\frac{\pi}{6} D^3}\right) \qquad [8]$$

The liquid film on the grain boundaries inside the particles is assumed to be relatively small compared to the grain size G; thus,

$$V_B = S_G \left(\frac{\delta}{2}\right) F_C n_G \qquad [9]$$

with S_G being the surface area per grain, $\delta/2$ being the width of the grain boundary film assigned to each grain, F_C being the fractional grain boundary coverage by liquid ($0 \le F_C \le 1$), and n_G being the number of grains per particle. Most important is the fractional coverage of grain boundaries by liquid, because this determines particle rigidity. It is determined by the quantity of liquid, the grain size, and its thickness on grain boundaries. Initially, before liquid formation, the number of grains per particle varies with the cube of the grain size to particle size ratio:

$$n_G = \left(\frac{D}{G}\right)^3 \qquad [10]$$

assuming the approximate grain volume is $V_G = G^3/2$. At high liquid contents, the grain boundaries are wetted by liquid and the film thickness on the grain boundaries contributes to the total volume. As liquid spreads on the grain boundaries, Eq. [10] is modified to give an approximate solution for the volume of liquid and solid associated with each grain V_G as

$$V_G = \frac{(G + F_C\delta)^3}{2} \approx \frac{1}{2}(G^3 + 3G^2 F_C \delta) \qquad [11]$$

Accordingly, the number of grains becomes

$$n_G \approx \frac{D^3}{G^2 (G + 3F_C\delta)} \qquad [12]$$

A substitution of $S_G \approx 3G^2$ into Eq. [9] gives

$$V_B = 1.5\ F_C\ \delta\ G^2\ n_G \quad [13]$$

as the volume of boundary liquid per particle.

The volume of liquid per particle located at the necks between particles depends on the neck size, as measured by X in Figure 4; thus,

$$V_N = \frac{\pi}{4} X^2 \left(\frac{\delta}{2}\right) F_C\ N_P \quad [14]$$

where F_C is the fractional coverage and N_P is the particle packing coordination. From measurements on quenched microstructures, it was determined that the coverage and dimensions of the liquid located at the necks during densification are the same as the grain boundary wetting, and the liquid necks are the same size as the grains. Based on these observations, the neck size approximates to the grain size to give

$$V_N = \frac{\pi}{8} G^2\ \delta\ F_C\ N_P \quad [15]$$

The particle packing coordination number N_P varies with the fractional density ρ for the system and can be empirically estimated for sintering structures as follows:[14]

$$N_P = 14 - 10.4\ (1 - \rho)^{0.38} \quad [16]$$

Because the particles remain essentially spherical, but the grains are shape accommodated, there is a difference in the coordination numbers (Eq. [7] *vs* Eq. [16]).

The quantity of liquid at the grain interior is assumed to remain a constant fraction of the total liquid V_L,[5]

$$V_I = F_I V_L \quad [17]$$

where F_I is a the fraction of liquid at the grain interior ($0 \le F_I \le 1$). It depends on the details of the powder microstructure, as dictated by the composition and atomization process.

A combination of Eqs. [13], [15], and [17] gives the liquid volume as follows:

$$V_L = F_I V_L + G^2\ \delta F_C\ (0.4\ N_P + 1.5\ n_G) \quad [18]$$

Equation [18] can be regrouped to give

$$V_L = \frac{G^2\ \delta\ F_C}{1 - F_I}\ (0.4\ N_P + 1.5\ n_G) \quad [19]$$

Equation [19] provides an important relation between liquid volume in a particle, as estimated from the phase diagram, and the microstructural features.

IV. PERCOLATION CONCEPTS

During SLPS, the total solid fraction is dictated by the alloy composition and sintering temperature. The rheological response is set by the fluidity of the solid-liquid system. Above the solidus temperature, liquid films coat grain boundaries, resulting in a loss of strength.[15] If the grain boundaries are coated with liquid, then grain sliding occurs in response to the capillary forces. Alternatively, if the grain boundaries are solid, then the system rigidity retards densification. In this case, the effective viscosity is estimated from the diffusivity.[16] For a given liquid volume, there is a distinction between liquid that nucleates on grain boundaries *vs* interdendritic locations. Accordingly, the fractional coverage of liquid on grain boundaries, F_C, is a key parameter that determines the densification kinetics. Combining Eqs. [8] and [19] with some numerical approximations gives

$$F_C = \frac{(1 - \Phi)\ (1 - F_I)\ D^3}{\delta\ G^2\ (0.8\ N_P + 3\ n_G)} \quad [20]$$

realizing the fractional coverage is also related to the number of grains per particle, n_G.

During liquid formation and spreading, there is grain growth. Additionally, as expressed by Eq. [7], there is a change in the grain coordination number with an increase in the liquid volume fraction. Grains grow rapidly *via* diffusion through the liquid phase. Isothermal experiments generally show classic grain coarsening behavior:[11]

$$G^3 = G_0^3 + \kappa\ t \quad [21]$$

where G_o is the starting grain size and κ is the grain growth rate constant. Measurements of grain size just below the solidus *vs* in the two-phase solid-liquid region often give a 20-fold increase in the rate constant with liquid formation.[11] Further, the grain growth rate constant is sensitive to the liquid content. To account for these factors, a hybrid grain growth rate constant is applied to the SLPS problem,[14,17] resulting in the following form:

$$\kappa = (1 - F_C)\ \kappa_S + \frac{F_C\ \kappa_L}{(1 - \Phi)^{2/3}} \quad [22]$$

where F_C is the fractional coverage of grain boundaries, κ_S is the solid-state grain growth rate constant, κ_L is the liquid phase rate constant, and Φ is the solid volume fraction.

During melting and grain growth, initially, there is too little liquid to fully coat grain boundaries, so the liquid films remain thin until most of the boundaries are penetrated.

Subsequently, with an excess of liquid over that needed to coat the boundaries and necks, the grain boundary film coarsens with further melting and grain growth.[7] In typical liquid-phase sintering systems, the grain growth rate constant is in the range of a 0.1 to 100 $\mu m^3/s$. Experiments with a boron-doped austenitic stainless steel during SLPS found κ in the range of 50 to 70 $\mu m^3/s$.[11] Accordingly, the change in grain size is relatively rapid during SLPS, thereby significantly affecting the fractional grain boundary coverage by liquid. The primary effect is through the decreasing number of grains per particle, leading to increased coverage of the remaining grain boundaries, even under isothermal conditions. Thus, grain growth is very important in determining the fractional coverage of grain boundaries by liquid, and in turn, this affects viscosity.

Percolation concepts are important in determining the onset of viscous flow of the semisolid particles. If a high level of solid grain bonding exists, then the system is rigid and no densification occurs. Alternatively, if no bonding occurs, there is loss of rigidity and compact shape. The relation between the microstructural connectivity and viscous flow is given by the critical condition for loss of a percolated structure,[5]

$$N_G\ P_C = C_N \quad [23]$$

where C_N is the critical number of connections, N_G is the

Table I. System Behavior and Classification

Region	State	Approximate Solid Content	Typical Fractional Coverage	Behavior
I	solid	1.00	0.00	minimal densification, solid state
II	rigid	0.95 to 1.00	0.00 to 0.70	slow, diffusional creep
III	mushy	0.75 to 0.95	0.70 to 0.80	viscous flow, high viscosity
IV	semisolid	0.60 to 0.90	0.80 to 0.90	rapid densification by viscous flow
V	fluidlike	<0.60	1.00	shape loss
VI	liquid	0.00	—	fluid

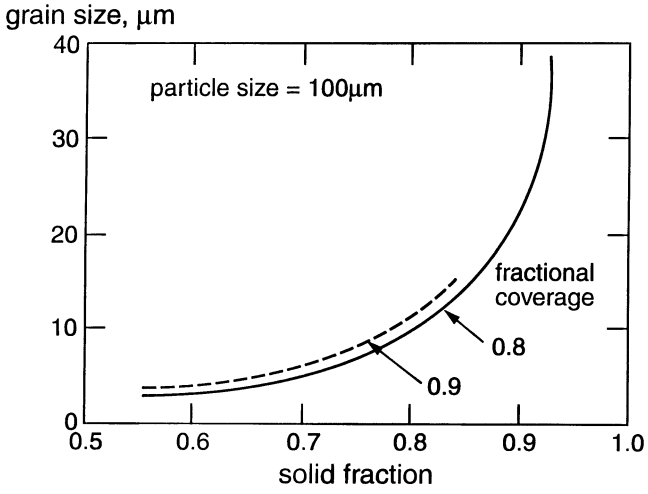

Fig. 5—Calculated combinations of grain size G and fractional coverage F_C of grain boundaries by liquid as functions of the solid content of Φ for 100-μm particles.

grain coordination number, and P_C is the probability of a connection between two contacting grains. Assume a simple relation between F_C, the fractional grain boundary coverage, and P_C:

$$P_C = 1 - F_C \qquad [24]$$

For loss of a percolated structure, C_N is approximately 1.5, which is the condition for the formation of a semisolid structure.[5] Thorpe[18] shows an intermediate case between rigid and semisolid, termed the ''mushy condition.'' This occurs when C_N is 2.4, leading to the possibility of six states during heating, as introduced in Table I. Supersolidus liquid phase sintering occurs in region IV, when the fractional coverage is high, but less than unity. Note the solid volume fraction probably ranges from 0.6 to 0.9 in this stage.

For the initial grain structure, with approximately 14 neighbors for each grain (tetrakaidecahedron), the condition in which rigidity is lost occurs when $F_C = 0.89$, or 89 pct of the grain boundary area is covered with liquid. At this point, the semisolid system lacks long-range connectivity and acts as a high viscosity structure. For the intermediate case of a mushy system, the corresponding fractional coverage is slightly less at 0.83. However, as temperature increases and more liquid forms, the grains grow and decline in coordination number, as expressed in Eq. [7]. Prior reports of SLPS show about 30 vol pct liquid is typical for densification, which gives $N_G = 9.0$ (Eq. [7]) and $F_C = 0.73$ (Eqs. [23] and [24]) for the onset of a mushy condition and $F_C = 0.83$ for loss or rigidity. Thus, as outlined in Table I, the fractional coverage of grain boundaries identifies the semisolid condition that gives densification. However, once the fractional coverage reaches unity, there is an inability to retain compact shape during sintering.

Depending on the microstructural conditions, the onset of viscous flow densification corresponds to widely differing liquid contents, as illustrated in Figure 5 for a particle size of 100 μm. Shown are the combinations of grain size and solid content corresponding to fractional coverages of 0.8 and 0.9. During heating, the solid fraction is declining and the grain size increasing. Thus, most typically, the heating trajectory eventually passes the critical condition, in which the particles become semisolid and densification occurs. If conditions are sustained where F_C is small, such as 0.8, then densification is slow. However, more typically, grain growth occurs and the fractional coverage continuously increases, even for a low liquid content, eventually leading to sufficiently large grains to give a high coverage of grain boundaries. One of the puzzles concerning SLPS has been an inability to explain densification on the basis of liquid content. The puzzle is explained by noting that differing initial microstructures and grain growth rates lead to different intersections of the heating pathway with the critical conditions, as illustrated by Figure 5.

V. CAPILLARITY

The liquid at the interparticle neck provides a capillary force that induces neck growth and densification. Viscous flow is one of the more widely treated mechanisms of sintering.[14] The capillary stress during SLPS has been the subject of a recent analysis.[8] The capillary stress was determined as a function of the sintering shrinkage, contact angle, particle size, and liquid content. Based on model behavior for two spheres of diameter D, the contact stress σ across the bond between particles is estimated as follows:

$$\sigma = \frac{5.2\ \gamma_{LV} \cos(\theta)}{D\left(\frac{\Delta L}{L_0}\right)} \qquad [25]$$

where γ_{LV} is the liquid-vapor surface energy, θ is the wetting angle (assumed to be zero), and $\Delta L/L_0$ is the sintering shrinkage. The maximum shear stress is one-half the contact stress. It is the shear stress at the particle bonds that drives sintering densification in SLPS.[9]

VI. VISCOUS FLOW

The viscosity of a semisolid particle is a novel rheological problem. There is a yield strength because the solid structure starts as a rigid, connected microstructure. As liquid spreads on the grain boundaries, the yield strength de-

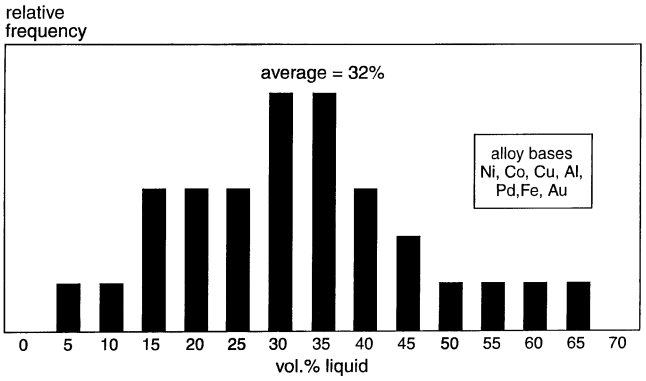

Fig. 6—A bar chart showing the distribution in previously reported optimal liquid contents for sintering densification of prealloyed powders with a mean of 32 vol. pct liquid.

clines rapidly above the solidus temperature. Yield strengths of semisolid systems have been reported over a wide range from 0.01 kPa to 100 MPa.[15,19,20] The sintering capillary stress is typically near 1 MPa. As liquid spreads on grain boundaries and particle necks, the yield strength declines and the rheological behavior shifts to that of a loaded suspension. This is the opposite of the situation encountered in casting, where the mixture starts as pure liquid and progressively increases in viscosity. In the condition in which densification occurs, the viscosity converges toward that encountered in highly filled polymers or after stirring in rheocasting.[20–26] As the pores are filled, the loss of porosity reduces the densification rate to zero.

Based on studies of semisolid alloys, there are solid content and strain rate effects on the viscosity.[19,23,27,28] Further, the yield strength depends on the shear strain rate and solid content. At high liquid contents, the behavior converges toward Newtonian viscous flow with a small or nonexistent yield strength. A fit to available data shows that the yield strength τ_Y variation with solid fraction Φ can be approximated as

$$\tau_Y = \tau_0 (\Phi - \Phi_Y) \qquad [26]$$

where Φ_Y is the solid content corresponding to loss of strength and τ_0 is the alloy strength just prior to liquid formation. For lead-tin alloys, Φ_Y is near 0.3.[19] However, in correlations with sintering distortion observations on tool steels[29] and nickel-based alloys,[10,11] a value near 0.6 is more reasonable for SLPS. This same value was observed in the settled solid volume fraction forming a skeletal structure in liquid-phase sintering systems.[17] Above this solid content, the yield strength progressively increases, but the system strength is generally less than the sintering stress, meaning that τ_0 is probably near 1 MPa. Based on the observations by Wang and Raj,[30] a Bingham response is assumed here:

$$\tau - \tau_Y = \eta \frac{d\gamma}{dt} \qquad [27]$$

where τ is the capillary-induced shear stress, τ_Y is the yield stress, η is the apparent viscosity, and $d\gamma/dt$ is the shear strain rate. In the range in which SLPS occurs, a realistic yield strength is below 1 MPa. Calculations for various assumptions of Φ_Y (from 0.3 to 0.6) and τ_0 (from 0.01 to 1 MPa) determined that the densification temperature was not sensitive to these parameters.

The viscosity of a semisolid particle depends on several factors. Rheological models were assessed for rheocasting, solder pastes, filled polymers, cements, superplastic glass ceramics, and liquid-phase sintering.[5,19–33] Based on earlier models[5,9,22] as adapted to the conditions where the fractional grain boundary coverage by liquid allows viscous flow, the apparent viscosity is calculated as follows:

$$\eta = \frac{\eta_0 G_0^3}{G^3 \left(\frac{d\gamma}{dt}\right)^m} \exp\left(\frac{Q}{RT}\right) \frac{(\tau - \tau_Y)}{\left(1 - \frac{\Phi}{\Phi_C}\right)^2} \qquad [28]$$

where η_0 is a combination of factors that includes numerical constants, the liquid viscosity pre-exponential, and a grain agglomeration factor; G_0 is the normalized grain size characteristic to the rheocasting measurements; Q is the activation energy for viscous flow; R is the gas constant; T is the absolute temperature; m is the strain-rate-sensitivity exponent; and Φ_C is the critical solids loading for viscous flow. When the solid content is above the critical level, the system strength resists viscous deformation.

From prior reports with loaded systems, rheocasting alloys, and SLPS alloys, it is evident that Φ_C depends on several factors, including F_C. From Eqs. [20], [22], and [23], the critical solids loading for the onset of viscous flow is calculated to range from 0.9 to 0.6 for most cases. Figure 6 plots the range of solid contents reported for optimal densification from prior studies.[3] These data exhibit a wide variation with a mode solid content of 0.7. No deagglomeration factors are included in this model, although prior studies on semisolid systems note a viscosity decrease over time from grain deagglomeration.[33]

Prior reports provide guides to the values of these parameters. For example, the viscosity of many pure metals is near 5 MPa· s,[34] with Q usually between 5 and 50 kJ/mol. The strain-rate-sensitivity m is usually between 0.7 and 1.0[5,19,27,28,30] and is assumed to be unity for these calculations. Accordingly, apparent viscosity data were evaluated using semisolid extrusion and rheocasting data, giving

$$\frac{\eta_0 G_0^3}{\left(\frac{d\gamma}{dt}\right)^m} = 10^{-14} \text{ m}^3 \text{ s} \qquad [29]$$

This estimate arises because the sintering densification rate usually peaks at equivalent strain rates between 10^{-2} and 10^{-3} s^{-1}, while rheocasting data are often gathered at much higher strain rates. Likewise, grain sizes for rheocasting data typically are in the 100- to 250-μm range (*vs* 2 to 40 μm for SLPS). Most metallic liquids have pre-exponential viscosity terms near $0.3 \cdot 10^{-3}$ Pa · s. Thus, Eq. [29] is an approximation that is needed, because the existing rheological data must be extrapolated over a wide range from the strain rates and grain sizes typical to rheocasting conditions to the smaller grain sizes and lower strain rates encountered in SLPS.

Equations [20], [24], and [25] provide a base for calculation of Φ_C. For example, a Pb-Sn solder at 42 vol pct solid has an apparent viscosity below 1 Pa · s[19] at a shear rate of 230 s^{-1}, while a Cu-Al alloy at 50 vol. pct solid has an apparent viscosity in the range from 0.5 to 10 Pa · s,

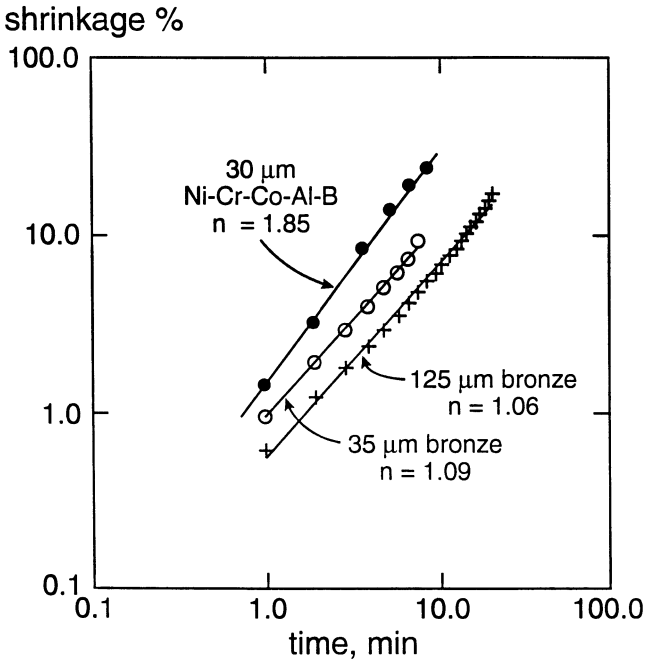

Fig. 7—Sintering shrinkage *vs* time as measured using dilatometry for three powders to test the theoretical expectation of a log-log slope of slightly over 1.

depending on shear rate.[27] When adjusted for the typical conditions associated with SLPS densification, the predicted viscosities are near 1 MPa · s.

VII. DENSIFICATION

Densification by viscous flow starts with a fractional coverage of the grain boundaries near 0.73 and is complete before it reaches 0.90. Viscous flow sintering of rods and spheres is a popular topic of theoretical and numerical treatments.[14,35–41] The models exhibit slight differences in details, but largely confirm Frenkel's assessment that shrinkage increases linearly with isothermal time. Neck size grows with approximately the square root of time. Liu *et al.*[8] give detailed analysis of the relations between neck size, shrinkage, and capillary force for a range of contact angles and liquid contents in SLPS.

Based on the finite element analysis of viscous flow sintering by Jagota and Dawson[40] and the supersolidus sintering relations by Liu *et al.*,[9] it is concluded that shrinkage during isothermal sintering $\Delta L/L_0$ is given as

$$\frac{\Delta L}{L_0} = \frac{\gamma_{LV}\, t}{D\, \eta} \qquad [30]$$

where γ_{LV} is the liquid-vapor surface energy, η is the semisolid apparent viscosity, t is the sintering time, and D is the particle diameter. Equation [30] is valid for shrinkages up to 10 pct. Tests of this model in SLPS have demonstrated reasonable agreement. Figure 7 is a log-log plot of sintering shrinkage *vs* time for a nickel-base alloy powder and two bronze powders. The slopes are 1.85, 1.06, and 1.09, while the prediction would be a slope of 1. In other tests using dilatometry, slopes of 1.02, 1.25, 1.28, 1.15, and 1.45 were measured.[9,11] Because the average time dependence is an exponent close to 1.3, Eq. [30] is a lower limit approximation.

If the sintering shrinkage and starting green density are known, then the sintered density can be calculated assuming constant mass and isotropic shrinkage. The sintered density for a compact starting at a fractional green density ρ_G is given as

$$\rho = \frac{\rho_G}{\left(1 - \frac{\Delta L}{L_0}\right)^3} \qquad [31]$$

where ρ is the fractional sintered density.

Closed pores form at densities between 85 and 95 pct of theoretical. Measurements on pore closure during SLPS processing of nickel superalloys determined that the first closed pores form at 85 pct density.[42] Half of the pores are closed by 90 pct density, and all of the pores are closed by 94 pct density. Final stage densification depends on the continued collapse of these spherical pores. Various models have been proposed for this problem.[14,43,44] Generally, if the pores are free of gas, this final phase of densification is relatively fast because of the increasing capillary pressure as the pore size decreases. As densification occurs, there is approximately one pore per particle, giving an approximation for the pore size d_P *vs* the particle size D and sintered fractional density ρ:

$$d_P = D\left(\frac{1-\rho}{\rho}\right)^{1/3} \qquad [32]$$

As an example, for a fractional density of 0.92, this gives a pore size to particle size ratio (d_P/D) of 0.44, assuming no pore coarsening.

The driving stress for final stage viscous flow sintering is the surface tension of the spherical pore, less the internal pressure from trapped gas:

$$\sigma = \frac{4\ \gamma_{LV}}{d_P} - P_g \qquad [33]$$

where γ_{LV} is the liquid-vapor surface energy and P_g is the gas pressure in the closed pore. As the pore shrinks, the higher stress accelerates densification, but any simultaneous pore coarsening or gas pressurization retards densification.[45] A final stage densification model for a viscous system is constructed from prior works.[16,43,44] For densities over 0.9 (the point of pore closure), gas pressurization during pore closure leads to progressively slower pore shrinkage:

$$\frac{dd_P}{dt} = \frac{1}{\eta}\left(4\ \gamma_{LV} - d_P\, P_g\right) \qquad [34]$$

When the gas pressure is known during sintering, the final density is estimated assuming no solubility of the gas in the sintering material. More complicated cases involving soluble gases are treated elsewhere.[45] The pore size at the onset of the final stage sintering is given by Eq. [32], designated as d_{PF}. Subsequently, the pore size is limited by gas pressurization:[14]

$$d_P = \left(\frac{d_{PF}^3\, P_g}{4\ \gamma_{LV}}\right)^{1/2} \qquad [35]$$